

Development of an ECM-mimetic, Electrospun Hydrogel Scaffold for Soft Tissue Repair

Application

by

Chongji Liu

A Thesis Presented in Partial Fulfillment
of the Requirements for the Degree
Master of Science

Approved July 2014 by the
Graduate Supervisory Committee:

Stephen Massia, Chair
Vincent Pizziconi
Christine Pauken

ARIZONA STATE UNIVERSITY

August 2014

ABSTRACT

The objective of this research is to develop a biocompatible scaffold based on dextran and poly acrylic acid (PAA) with the potential to be used for soft tissue repair. In this thesis, physical and chemical properties of the scaffold were investigated. The scaffolds were made using electrospinning and cross-linked under high temperature. After heat treatment, Scanning Electron Microscope (SEM) was used to observe the structures of these scaffolds. Fourier transform infrared spectroscopy (FTIR) was used to measure the cross-linking level of scaffold samples given different times of heat treatment by detecting and comparing the newly formed ester bonds. Single-walled carbon nanotubes (SWCNT) were added to enhance the mechanical properties of dextran-PAA scaffolds. Attachment of NIH-3T3 fibroblast cells to the scaffold and the response upon implantation into rabbit vaginal tissue were also evaluated to investigate the performance of SWCNT dextran-PAA scaffold. SEM was then used to characterize morphology of fibroblast cells and rabbit tissues. The results suggest that SWCNT could enhance cell attachment, distribution and spreading performance of dextran-PAA scaffold.

DEDICATION

This thesis is dedicated first to my father Shenguo Liu, my mother Shuying Li and my sister Rui Liu for their persistent encouragement and support whenever I met difficulties and obstacles.

ACKNOWLEDGMENTS

I would like to express my deepest appreciation to my mentor, Professor Stephen Massia. Without his guidance and help, I could not have finished this thesis.

I want to thank Dr. Vincent Pizziconi and Dr. Christine Pauken for your support and guidance. Thank my friends Kimia Seyedmadani, Nathan Baldwin and Robert Espinoza for your help and assistance on my thesis.

I also thank Dr. Jeffrey Cornella and Dr. Johnny Yi from Mayo Clinic, Scottsdale, AZ for their support and assistance on this research.

Many thanks to Mr. Karl Weiss, Mr. Kenneth Mossman, Mr. Sisouk Phrasavath and Mr. Zhenquan Liu for the assistance of using material science facilities in LeRoy Eyring Center for Solid State Science. I would also like to thank David Lowry for the assistance of using facilities in Life Sciences Electron Microscopy (EM) Laboratory.

TABLE OF CONTENTS

	Page
LIST OF TABLES	v
LIST OF FIGURES	vi
CHAPTER	
1 INTRODUCTION	1
Soft Tissue Repair	1
Electrospinning.....	2
Parameters in Electrospinning	5
Mechanical Properties.....	6
Application of Carbon Nanotubes to Biomaterials	7
Cell-material Interaction	8
Scaffold for Pelvic Organ Prolapse (POP) Treatment	9
2 PROJECT HYPOTHESIS AND SPECIFIC AIMS	11
3 MATERIALS AND EXPERIMENTAL METHODS	12
Materials	12
Electrospinning Solution Preparation.....	13
Electrospinning of Dextran-PAA Scaffold.....	13
Fibroblast Cell Seeding.....	14
Rabbit Implantation Test.....	15
Fibroblast Cell Phalloidin and DAPI Staining	15
Scanning Electron Microscope Observation	16
FTIR Measurement	17

CHAPTER	Page
4 RESULTS	18
Scaffold Thermal Cross-linking Analysis	18
FTIR Result Analysis.....	22
SWCNT Scaffold Structure Analysis.....	24
Cell Response to SWCNT Dextran-PAA Scaffolds	27
Cell Fluorescence Assay	29
Implantation of Scaffolds and Tissue Response Evaluation.....	32
5 CONCLUSION	36
REFERENCES.....	38
APPENDIX	
A SUPPLEMENT IMAGES.....	41

LIST OF TABLES

Table	Page
1. Literature Review of Electrospinning Materials	5

LIST OF FIGURES

Figure		Page
1.	Schematic of Electrospinning Systems	4
2.	Molecular Structure of Single-walled Carbon Nanotubes (SWCNT)	8
3.	Cell Culture Glass Cylinder	14
4.	1000X SEM Images of Dextran-PAA Scaffolds	19
5.	2500X SEM Images of Dextran-PAA Scaffolds	21
6.	Schematic of Esterification Between Dextran and PAA	23
7.	FITR Spectrum of Dextran-PAA Scaffolds	23
8.	Dextran-PAA Scaffolds with Different Concentrations of SWCNT	24
9.	SEM Images of Scaffolds with Different Concentrations of SWCNT	26
10.	SEM Images of Fibroblast Cells on Dextran-PAA Scaffolds	28
11.	Fluorescent Images of Fibroblast Cells on Dextran-PAA Scaffolds	31
12.	Scaffolds Wrapped Surgisis Graft before and after Rabbit Implantation ...	32
13.	Rabbit Tissue on Dextran-PAA Scaffolds after 14 days Implantation	35
14.	SEM Images of Surgisis Graft Surface	42
15.	3T3 Fibroblast Cells on Dextran-PAA Scaffold	43
16.	3T3 Fibroblast Cells on 0.01% SWCNT Dextran-PAA Scaffold	44
17.	3T3 Fibroblast Cells on 0.1% SWCNT Dextran-PAA Scaffold	45

CHAPTER 1

INTRODUCTION

Soft Tissue Repair

Many human tissues have a limited capability to regenerate once they are damaged. Even after surgeries, many functions do not return to the normal level. Much progress has been made in improving soft tissue repair since 1980s. One approach for soft tissue repair is to use ECM mimetic materials to direct tissue regeneration. The ECM is a complex scaffold secreted by cells and one of its most important functions is to provide structural support for its surrounding cells. The ECM not only provides physical structure and support, but also directs cell attachment, proliferation, differentiation and regeneration of cells in a tissue-specific manner. However, one of the biggest challenges for ECM mimetic scaffold development is how to design a scaffold has the same function as the underlying ECM to be replaced. There are many factors that need to be considered when designing a scaffold. First of all, the materials for scaffolds must be biocompatible and the products of their degradation must be non-toxic. An ideal scaffold should be able to degrade at a rate matching the formation of its surrounding new tissues. In addition, after implantation, the scaffold must be able to provide enough structural support for its surrounding tissues until the tissue ECM has formed [25]. Another basic requirement for ECM mimetic scaffold is it must be porous and therefore facilitate nutrient transportation and oxygen/carbon dioxide exchange. To achieve these requirements, scaffold development requires many areas of research from cell biology to chemical and physical characterizations. Studies to date have developed a variety of ECM mimetic scaffolds for different clinical applications. There are mainly two kinds of materials for scaffold

development, synthetic polymer and natural polymer materials. Synthetic polymer materials such as poly glycolic acid, poly lactic acid and poly vinyl alcohol have been investigated extensively for soft tissue repair applications. Natural polymer materials include proteins such as collagen, elastin and gelatin and the polysaccharides such as cellulose, hyaluronate, chitin, and alginate [26]. However, there are many limitations of natural material scaffolds due to their relatively poor mechanical properties [27] and unpredictable degradation rate. When compared with natural material scaffold, chemical and physical properties of synthetic material scaffolds can be well controlled, which make them more reproducible.

Electrospinning

In recent years, electrospinning technique has garnered much attention because of its ability to produce fibrous scaffolds, which can mimic the real ECM of human and animal tissues. The principle of electrospinning is to utilize an electric field to draw fine fibers with diameters in the range of nanometers to micrometers from polymer solutions. Electrospun scaffolds have shown several advantages compared to traditional hydrogel based scaffolds. First of all, electrospun scaffolds mimic the real ECM very well. The large surface/volume ratio of these electrospun nanofiber-based scaffolds provides the foundation for the attachment and proliferation of seeded cells. In addition, electrospun scaffolds facilitate cell infiltration and migration as well as oxygen and drug delivery due to their porosity. Moreover, electrospun scaffolds provide 3D mechanical support rather than 2D plane for cell and tissue formation and cell culture, which makes it possible to

construct 3D tissue structures. Both natural materials and synthetic materials can be electrospun into fibrous scaffolds. Most electrospun scaffolds require cross-linking treatment after electrospinning in order to form reliable chemical bonds to maintain the structural stability.

Generally, an electrospinning system is comprised of four necessary components: a polymer solution infusing system (including syringe and blunt tip needles), a pump to provide well controlled flow of polymer solution to ambient environment, a direct current power supply that provides a range of voltages to obtain the functional electrical gradient and a fiber collector (usually conductive materials like aluminum foils). Polymer droplets are formed when the solution is ejected out of the infusing system. A high voltage gradient controlled by the DC power supply is provided between the needle and fiber collector. Polymer droplet is charged when it is ejected out of syringe [23]. Once the repulsion within the droplet, caused by charge, overcomes the droplet surface tension, Taylor Cones [1, 2] will be formed. Polymer jet, following Taylor Cones, undergoes a process that results in the formation of long and fine fibers. In this process, the polymer solvent evaporates and solidifies when traveling in the air [20].

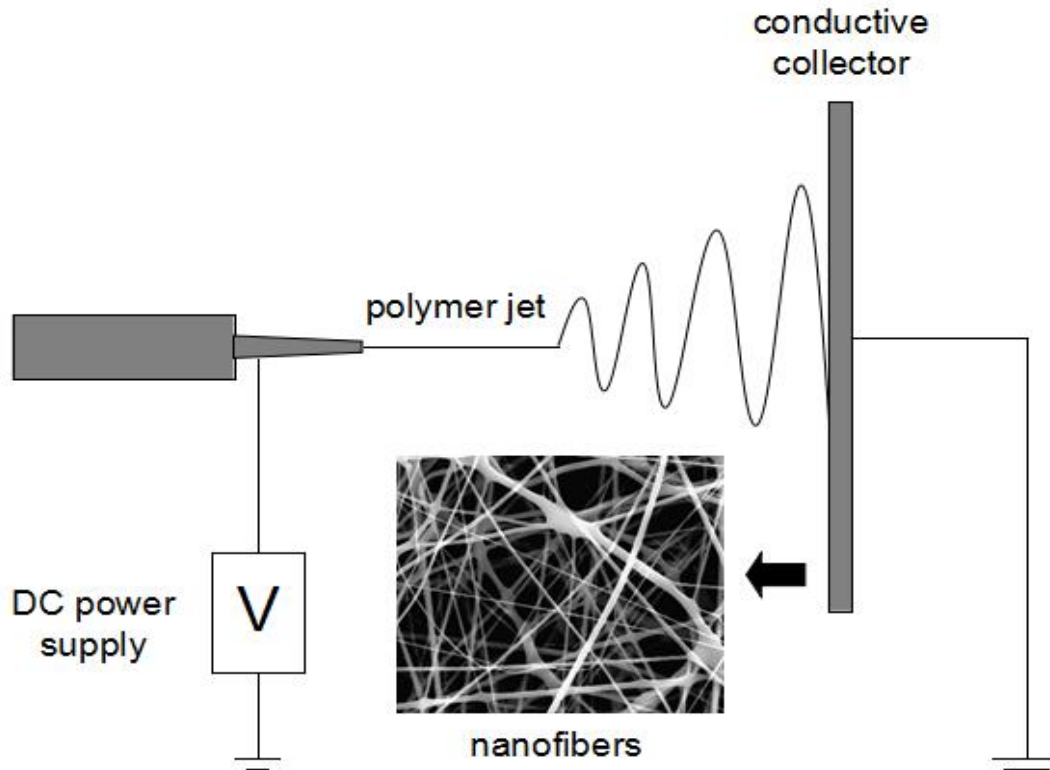


Figure.1 Schematic of Electrospinning Systems

According to previous research, more than fifty kinds of polymers have been successfully electrospun into fibers with diameter ranging from 3nm to 5 μ m (Table 1 lists some examples). Basically, polymer electrospinning can be divided into polymer solution electrospinning and polymer melt form electrospinning. Polymer solution electrospinning is most widely used to date since this process is relatively simple and straightforward. The polymer is first dissolved into solvent to form polymer solution. The polymer solution is then loaded into solution ejecting system for electrospinning. Most polymer solution electrospinning can be conducted at room temperature at controlled humidity range. In polymer melt form electrospinning, polymers are treated with heat to melt

instead of dissolving in solvents. The molten polymers are then electrospun into fibers.

Environment for melt electrospinning are stricter than solution electrospinning, usually in vacuum condition.

Polymer	concentration	Molecular Weight
Polyvinyl alcohol, PVA[3]	8%-16%	65K
Polylactic acid, PLA[4]	14%	205K
Polyethylene oxide, PEO[5]	7%-10%	400K
Silk[6]	12.5wt%	N/A
Type I collagen, Elastin[7]	1%-5%	N/A
poly vinyl phenol, PVP[8]	20%,60%	20K, 100K
Cellulose acetate, CA[9]	12.5-20%	N/A
Polyacrylamide, PAAM[10]	1-10wt%	5,000K
Poly(vinylidene fluoride) , PVDF [11]	20wt%	107K

Table 1 Literature Review of Electrospinning Materials

Parameters in Electrospinning

Electrospinning process can be influenced by a variety of parameters. These parameters include polymer solution properties like viscosity and surface tension, voltage applied between needle and collector, solution ejecting speed, processing temperature,

humidity and so on[12, 21]. These parameters directly control the electrospinning process and the properties of scaffolds such as fiber diameter, porosity and orientation. Therefore, by controlling these parameters, the final electrospun scaffolds can be controlled. Many researchers have investigated how each parameter influences the scaffold properties. For example, Fong H et al found that high viscosity of polymer solution cannot be electrospun into fibers because of the cohesiveness in the droplet. On the other extreme, beads will be formed instead of fibers when using solution of low viscosity for electrospinning[13]. So the microstructures of scaffolds are quite dependent on these independent processing parameters. In addition, for different polymers, even same polymers of different concentrations, processing parameters for the optimal electrospinning are necessarily different. As a result, each type of polymer solution used for electrospinning requires the determination of its unique processing parameters in order to produce qualified scaffolds. Thus, even though a variety of polymers can be used for electrospinning, a significant amount of development work is required to produce scaffolds to achieve demanded characters such as controllable diameters and porosity, bead-free scaffolds, uniformed and well distributed fibers, stiffness and many other design specification variables.

Mechanical Properties

Mechanical properties of scaffold for soft tissue repair are very important since they directly influence the cell attachment, proliferation and even differentiation. Engler et al showed that the phenotypes of stem cells are affected by the stiffness of scaffolds in which cells are attached [14]. Scaffolds for regenerative medicine use can mainly be

divided into bulk and nanofibers. For these two kinds of scaffolds, microstructures are totally different and this is why testing standards for these two are different. For bulk scaffold, usually hydrogel sheets, tests often include stiffness, hardness and many other mechanical properties. For nanofiber-based scaffolds, in addition to the test of stiffness and hardness on the whole scaffold substrate, single fiber tensile testing is also necessary. In general, extremely flexible scaffolds cause cell rounding up because they cannot support cell stretching while rigid scaffolds promote cell stretching and spreading [15]. Bulk mechanical properties of scaffolds, as well as, microstructural mechanical properties, have a significant impact on cell-material interactions. Therefore, controlling mechanical properties of scaffolds is key point in the achievement of a desired cell phenotype.

Application of Carbon Nanotubes to Biomaterials

Nanomaterials are promising in improving biomaterials due to their large surface area/volume ratios and the potential to manipulate the mechanical properties of biomaterials. Carbon nanotubes (CNT) are unique inorganic nanostructures consisting of hexagonal arranged carbon atoms. Carbon nanotubes can be divided into multi-walled carbon nanotubes (MWCNT), which have multiple graphene layers and single-walled carbon nanotubes (SWCNT), which are formed by rolling up a graphene sheet [16]. Despite the significant number of chemical and physical cross-linking methods have been investigated to achieve desired mechanical properties of electrospun scaffolds, they remain elusive and thus limit the application of a variety of biomaterials as structural scaffolds, especially hydrogel-based materials. CNT have been shown to improve

mechanical properties of hydrogels [17]. SWCNT were used to improve dextran-PAA scaffold's mechanical properties and cell and tissue response.

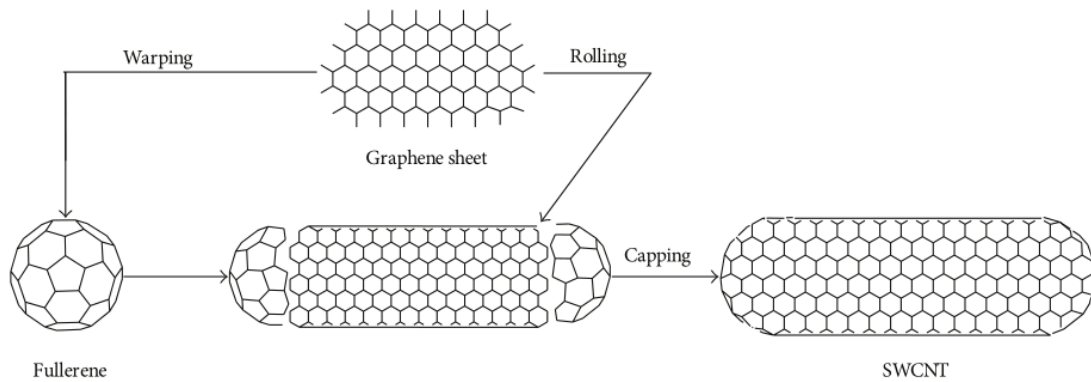


Figure.2 Molecular Structure of Single-walled Carbon Nanotubes (SWCNT) [16]

Cell-material Interaction

Studies to date suggest that one of the most pivotal design criterion to determine whether a scaffold will be qualified for clinical applications is its ability to achieve desired cell-material interaction. Cell-material interaction studies typically involve in a number of assays such as, cell proliferation, attachment, spreading and so on. In order to develop a scaffold for specific requirements, all these factors must be taken into consideration. Cell proliferation and tissue generation is a key factor when making scaffolds since the scaffolds for clinical applications should be able to promote cell proliferation and tissue generation. Cell attachment is another key issue in assessing a scaffold, especially for nanofiber-based scaffolds. Fiber diameter, porosity and stiffness are key factors that affect cell attachment. Ideal nanofiber-based scaffolds should be capable of forming desired cell attachment. Most polymers can fulfill the above two basic requirements, proliferation and acceptable cell attachment. However, it is more of a

challenge to achieve desired cell spreading on scaffolds, i.e., good cell morphology and ideal cell distribution. Cell spreading assessment is usually achieved through observations of cells on scaffolds using fluorescent microscopes and scanning electron microscopes. In tissue growth *in vivo*, cells make their own ECM and which associated chemical activity (signaling) provides feedback to stimulate cell spreading and migration. Ideal matrices of artificial polymer scaffolds should be able to mimic natural ECM to promote cell proliferation, attachment, migration and spreading. Significant efforts by many research groups have been devoted to improving cell-material interactions on scaffolds, but much research and development remains to achieve ideal scaffolds.

Scaffold for Pelvic Organ Prolapse (POP) Treatment

POP occurs when pelvic organs slip out or drop from their normal positions and result in a push against vaginal walls. Surgical treatment is widely used for POP, in which doctors physically reinforce the pelvic floor through implantation of surgical meshes. In the past few years, a large number of surgical meshes have been developed by medical device manufacturers such as Johnson& Johnson, Cook Medical and others. Until recently, a lot controversies have arisen due to the repair problems caused by these surgical meshes, which forced FDA to reevaluate the safety problems of these meshes. To date, FDA has ordered more than 40 mesh manufacturers to perform safety studies on their mesh products. In this preliminary research, we aim to develop a scaffold to improve the performance of surgical meshes and potentially eliminate the safety problems. As a result, surgical meshes not only provide physical support to pelvic organs, but also can promote regeneration of surrounding soft tissues and help them reconstruct

their own stable ECM. The physical and chemical properties of this scaffold were investigated. In addition, cell seeding assays and implantation into rabbit vaginas were also conducted to assess the performance of the scaffold.

CHAPTER 2

PROJECT HYPOTHESIS AND SPECIFIC AIMS

The objective of this research was to develop an ECM mimetic hydrogel scaffold using biopolymer dextran and synthetic polymer poly acrylic acid (PAA) and evaluate the cellular interactions *in vitro* and *in vivo*. Physical and chemical electrospinning conditions were determined to fabricate ECM mimetic scaffold. Single walled carbon nanotubes (SWCNT) were utilized to increase the mechanical stiffness of the scaffold. The effect of scaffold stiffness on cellular adhesion and spreading was evaluated. A second objective of this research was to use this scaffold for soft tissue repair and regeneration applications. This research focused on developing an implantable ECM mimetic scaffold to promote tissue repair for pelvic organ prolapse (POP).

It was hypothesized that electrospinning of dextran and PAA can form ECM mimetic scaffold that support cell attachment and tissue integration. To investigate this hypothesis, the following specific aims were established:

Aim 1: Develop the optimal electrospinning conditions for fabrication of dextran-PAA scaffold.

Aim 2: Develop thermal cross-linking conditions to optimize ECM mimetic structure and chemical stability of the scaffold.

Aim 3: Develop methods to increase the scaffold stiffness by incorporating carbon nanotubes into scaffold fibers.

Aim 4: Assess cell-scaffold interactions *in vitro*.

Aim 5: Evaluate tissue-scaffold interactions in a rabbit POP model.

CHAPTER 3

MATERIALS AND EXPERIMENTAL METHODS

Materials

Polymer materials used in this research for electrospinning are dextran and poly acrylic acid (PAA). Dextran has a good biocompatibility because of its low toxicity [21]. Besides, each unit of dextran contains three hydroxyl groups. These hydroxyl groups could be able to react with carboxyl groups to form ester bonds, which is produce stable, non-hydrolyzed scaffolds.

Dextran (500kD Mw) was purchased from Alfa Aesar (Ward Hill, MA). Poly acrylic acid (60kD Mw, 35wt% aqueous solution) was purchased from Polysciences, Inc (Warrington, PA). NIH-3T3 fibroblast cell was obtained from the American Type Culture Collection (ATCC). 21 gauge, 1.5 inch length stainless steel blunt needles for electrospinning were purchased from Small Parts, Inc. single-walled carbon nanotube (SWCNT) D1.5L1-5-COOH (diameter 1.5nm, length 1-5 μ m) was purchased from Nanolab. Inc (Waltham, MA). Glutaraldehyde (25 wt %) was purchased from Electron Microscopy Sciences (Hatfield, PA). Phalloidin (Alexa Fluor® 488 Phalloidin) and DAPI (4', 6-Diamidino-2-Phenylindole, Dihydrochloride) were purchased from Life Technologies (Carlsbad, CA). Surgisis pelvic floor graft (Cook Medical) was purchased remnants were obtained from Mayo Clinic Hospital (Phoenix, AZ). Surgical suture was purchased from Ethicon Inc. Phosphate-buffered saline (PBS, pH 7.0-7.2) was purchased from Thermo Scientific (Waltham, MA). DMEM (Dulbecco's Modification of Eagle's Medium) for 3T3 fibroblast cell culture was obtained from Corning Inc. (Corning, NY). PFA (paraformaldehyde, reagent grade, crystalline) for cell and tissue fixation and Triton

100X (laboratory grade) for cell staining were purchased from Sigma-Aldrich (St. Louis, MO).

Electrospinning Solution Preparation

For control scaffolds, which contain no bioactive molecules, 4 g of dextran and 3.6g PAA solution were added into 7.2ml DI water in 50ml tube. The mixture solution was rocked overnight until it became transparent yellow with no bubbles or solid lumps. The final concentration of the solution is 27 wt% dextran and 8.5 wt% PAA. To increase the mechanical stiffness of dextran-PAA scaffold, polymer solutions with 0.01%, 0.05%, 0.1%, 1% and 2% SWCNT were used for scaffold fabrication. 3.5% SWCNT solution was prepared and ultrasonicated using 25Hz power for 30 minutes at room temperature in order to decrease SWCNT agglomeration. Sonicated solutions were then added to dextran-PAA solutions to make 5 different concentration electrospinning solutions. After overnight shaking at room temperature, another 20 minutes ultrasonication was applied to the final SWCNT dextran-PAA polymer solutions before electrospinning.

Fabrication of Dextran-PAA Scaffolds

The dextran-PAA solution was loaded into 10ml syringe and then pumped out a metal needle with 9 micro-liter/min infuse rate under 15 kV voltage. Paper cards covered by aluminum foils were used as collectors and the distance between the needle and the collector was 18cm. Final volume of solution used for each electrospinning was 1ml. Cleaning was done during the electrospinning process every 10 minutes to make sure no

solidified polymer clog formed on the tip of needle. Scaffold samples were prepared using the same electrospinning parameters of voltage, distance, and solution volume and composition. The electrospun scaffolds were moved into desiccator for overnight drying to decrease the influence of water to cross-linking process. After overnight drying, the scaffolds were then cut into 1cm by 1cm pieces for thermal cross-linking. All the samples were placed into oven under 180°C for different time lengths from 15 minutes to 120 minutes. All the scaffold samples were then kept in the dry keeper before future use.

Fibroblast Cell Seeding

Scaffolds after thermal cross-linking treatment were used for cell seeding. 1 by 1cm scaffold pieces were placed into 24-well plates. Scaffold pieces were held flat on the bottom of wells using glass cell cloning cylinders. These cylinders can hold the cells on the scaffold pieces, therefore concentrate cell growth in the center areas of scaffolds (Figure.3). Scaffolds for SEM imaging was seeded with 250,000 cells per well. For fluorescent assays, 250,000 cells were seeded onto each scaffold. All the scaffolds were incubated for 8 days under 37°C.

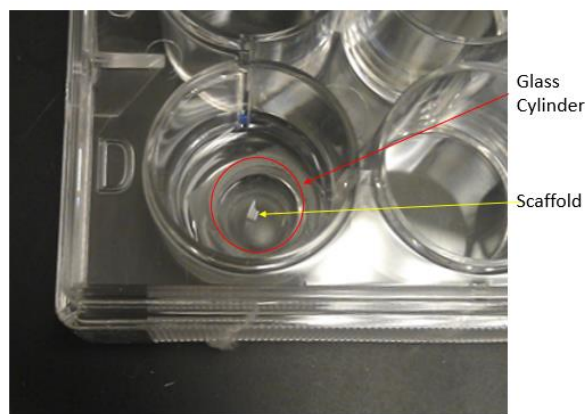


Figure.3 Cell Culture Glass Cylinder

Rabbit Implantation Test

To evaluate tissue-scaffold interactions in a rabbit POP model, adult New Zealand female rabbits weighting 3-6kg were used for scaffold implantation test. Rabbit implantation procedures used in this research were developed by Dr Jeffrey Cornella at Mayo Clinic (Phoenix, AZ) [28, 29]. All the surgical procedures were carried out at Mayo Clinic, Scottsdale, AZ. Rabbits were anesthetized and maintained under ventilation. The posterior vaginal wall was incised (a 4-cm longitudinal incision, beginning at the introitus), and bilateral vaginal flaps were dissected laterally to a distance of 1.0 cm to expose the rectovaginal fascia. 4.0 x 1.0 cm strip of scaffolds warped Surgisis grafts (grafts were sterilized using 75% ethanol before surgery. Cross-linked scaffolds with different concentrations of SWCNT were cut into 5.0 x 1.0 cm strips and wrapped around the Surgisis graft with a 2mm distance between each other) was then placed in the midline overlying the rectovaginal fascia and sutured in place at the distal end with a permanent, monofilament 5-0 suture. The vaginal incision was then be closed over the graft with interrupted sutures. Two rabbits were used for the 14-day implantation test. Surgisis grafts were taken out from rabbit after 14 days. The rabbit tissue samples were then fixed by glutaraldehyde at room temperature and treated using critical point drying (CPD). SEM imaging was utilized then to observe the rabbit tissue morphology on the grafts.

Fibroblast Cell Phalloidin and DAPI Staining

Cell attachment and spreading on dextran-PAA scaffolds were measured by Phalloidin and DAPI staining viewed by fluorescent microscope. Alexa Fluor 488

Phalloidin was used, which can be excited by 495nm wavelength excitation and emit 518nm light (green). DAPI has a maximum absorption at 358nm wavelength and can emit 461nm light (blue). Approximately 250,000 3T3 fibroblast cells were seeded onto each scaffold in a 24-well plate. After 8 days culture, the scaffolds were transferred to PBS medium before cell staining in order to eliminate the signal influence of unattached cells. After PBS medium rinsing, 4% PFA, PBS solution was used to fix the cells on the scaffolds for 15 minutes. The samples were then pretreated with 0.1% Triton 100X for another 15minutes. After PBS rinsing, 200 μ L of 2.5v/v% phalloidin, PBS solution was added to the each well to for 20 minutes stain the filamentous actin in fibroblast cells. DAPI PBS solution with a concentration of 4 μ L/1mL was then used to stain the DNA of fibroblast cells. After PBS rinsing, all the samples were imaged using Leica Microscope.

Scanning Electron Microscope Observation

After heat treatment, scanning electron microscope (SEM) was used to observe the structures of the scaffolds samples. SEM imaging was performed using an FEI XL-30 EFSEM on electrospun scaffolds that were sputter-coated with gold palladium. Scaffolds seeded using NIH-3T3 fibroblast cells were observed using JEOL JSM6300 SEM. Cell seeded samples were first fixed using 2% glutaraldehyde for 2 hours at room temperature and then dehydrated by acetone gradient treatment of 20%, 40%, 60%, 80% and 100%. Critical point drying (CPD) was then used to treat the acetone dehydrated scaffolds. This procedure protected the surface structure of the biological samples from the damage of

vacuum environment during SEM imaging. The samples were then sputtered with gold-platinum alloy before SEM imaging.

FTIR Measurement

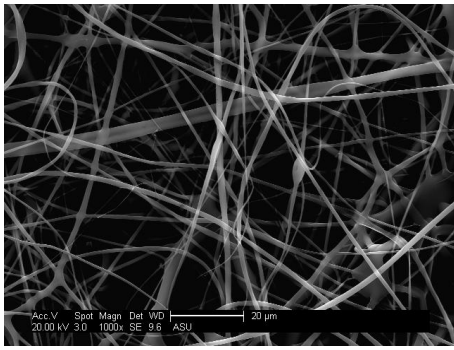
Fourier transform infrared spectroscopy (FTIR) (Bruker IFS 66V/S) and attenuated total reflectance Fourier transform infrared spectroscopy (ATR-FTIR) were used for chemical characterization of scaffolds. Dry scaffolds were measured using FTIR and hydrogel scaffolds were measured using ATR-FTIR. Mid-IR beam source was used since wavenumber range involved in this research is 800-4200 cm^{-1} . Auto baseline corrections were applied to the final data and Microsoft Excel was used for data plotting.

CHAPTER 4

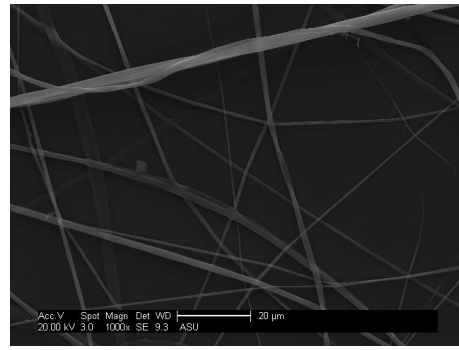
RESULTS

Scaffold Thermal Cross-linking Analysis

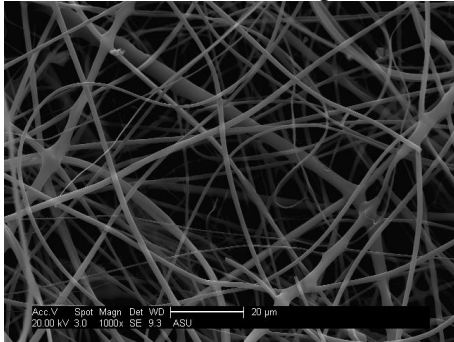
After the dextran-PAA scaffolds produced through electrospinning, the fibrous structures were formed. The scaffolds were quite unstable and they dissolved immediately in aqueous condition. In order to keep the scaffold structure stable in aqueous conditions without dissolving, chemical cross-linking is needed. In this research, thermal cross-linking method was utilized to treat the scaffolds after electrospinning. Scaffolds were dried in the desiccators overnight before heat treatment. Thermal cross-linking was done at 180°C, which has been proved effective to dehydrate the scaffolds [19]. The influence of heat treatment time on scaffold fibrous structure was investigated using SEM imaging. According to Figure.4, 180°C heat treatment for different time lengths, the fibrous structures of scaffolds are consistent and no discernible differences can be found when heat treatment times less than 60 minutes. But tiny changes happened when heat treatment time arrived to 60 minutes or greater, the fibrous structures of scaffolds began to ‘melt’ and fuse together. Even the diameter of a single fiber diameter varied. So based on the observation of these SEM images, we assume that the scaffold structure changes occur between 60 minutes and 80 minutes during 180°C heat treatment.



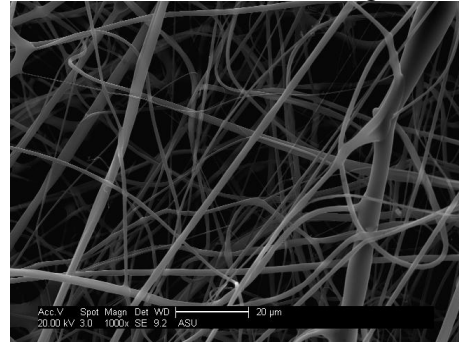
Pre cross-linking



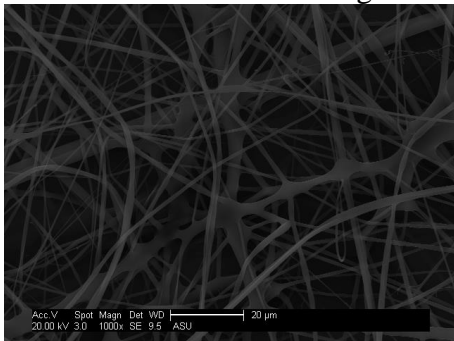
20min cross-linking



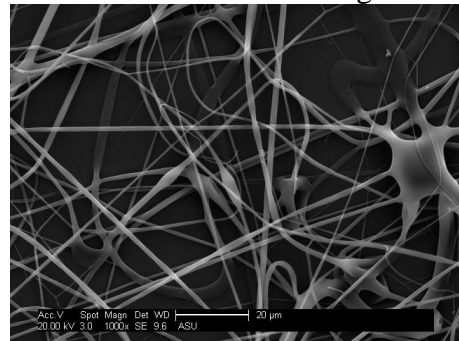
40min cross-linking



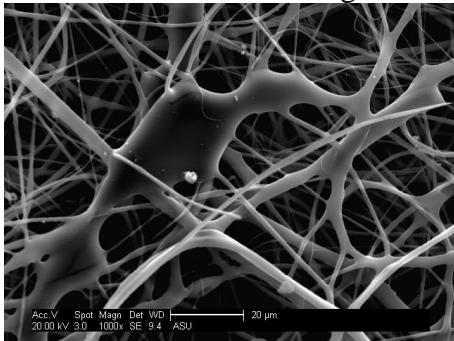
60min cross-linking



80min cross-linking



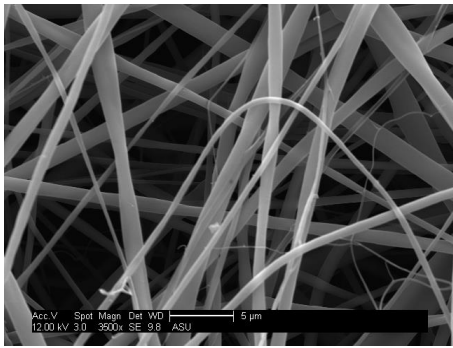
100min cross-linking



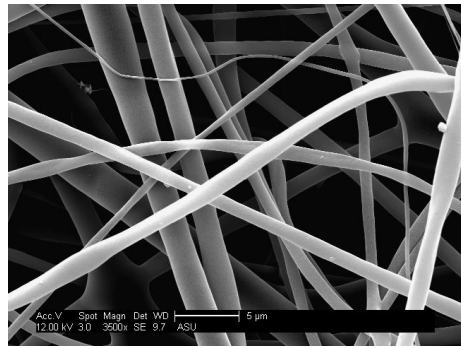
120min cross-linking

Figure.4 1000X SEM Images of Dextran-PAA Scaffolds

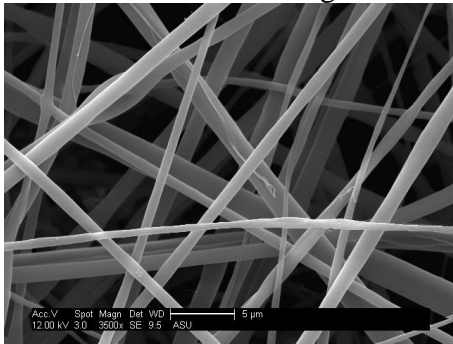
In Figure.5, images were taken in magnification of 2500X. Information on single fiber structure changes can be revealed from these higher magnification images. In the images which cross-linking time below 60 minutes, single fibers diameter vary very little. While when the cross-linking time over 60 minutes, deformation of fibers occurred and as heat treatment time increased, the deformation became more and more clear. In the images of scaffolds cross-linked for 80 minutes, some fibers fused together. With increased heat treatment time, more deformations and melt can be seen in SEM images. The result is consistent to Figure.4. Heat treatment could influence the fibrous structures of scaffolds when treatment time higher than 60 minutes. So in the rest of the experiments, 180°C, 60 minutes heat treatment was applied to the scaffolds in order to decrease the influence of heat to the structure of scaffolds.



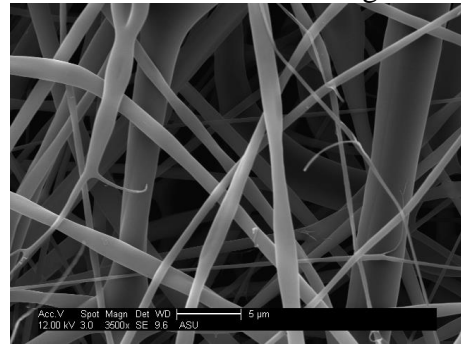
Pre-cross-linking



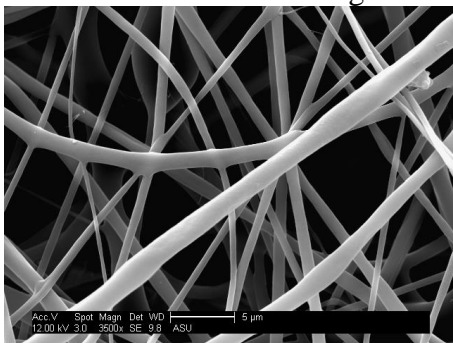
20min cross-linking



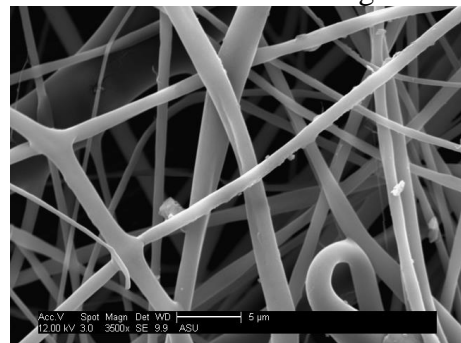
40min cross-linking



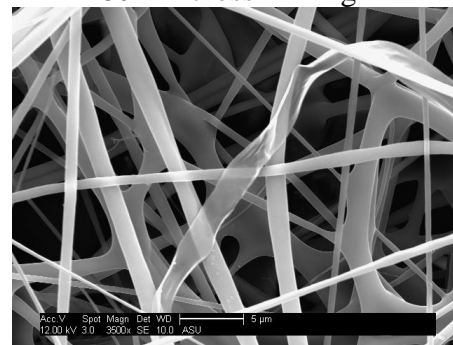
60min cross-linking



80min cross-linking



100min cross-linking



120min cross-linking

Figure.5 2500X SEM Images of Dextran-PAA Scaffolds

FTIR Result Analysis

In order to investigate the chemical reactions during the scaffold thermal cross-linking, FTIR was used. By comparing the peaks of functional groups on the spectrum, we can get an insight of the chemical reactions after heat treatment. In Figure.7, there is a clear increasing trend in both peaks between $1000-1100\text{ cm}^{-1}$ and between $3200-3500\text{ cm}^{-1}$. The increase in peak height between $1000-1100\text{ cm}^{-1}$ can be attributed to the newly formed C-O-C stretching vibration, which is caused by the reaction between the carboxyl group of PAA and hydroxyl group of dextran (Figure.6). This peak in $1000-1100\text{ cm}^{-1}$ is the main indicator to determine the cross-linking level of scaffolds. Ester bond was formed between dextran and PAA during 180°C heat treatment, which helped the scaffold maintaining its fibrous structure from dissolving in aqueous condition. The increase in peak height between $3200-3500\text{ cm}^{-1}$ is attributed to the newly formed hydroxyl group, which is produced by the degradation of unreacted carboxyl groups. Based on FTIR result, we assume that within a certain range, the cross-linking level of these dextran-PAA scaffolds as determined by the esterification of PAA and dextran, is positively correlated to the heat treatment time. Longer heat treatment helps to form more ester bonds and therefore produce more stable scaffolds. According to the FTIR result shown in Figure.7, there is obvious height increase on the peak within $1000-1100\text{ cm}^{-1}$ wavenumber. The degradation test of scaffolds in water at room temperature shows that 60 minutes cross-linked scaffolds were stable with no discernable dissolving after 45 days. According to the scaffold structure analysis result, heat treatment time over 60 minutes causes deformation to scaffolds, which potentially change their original fibrous structures.

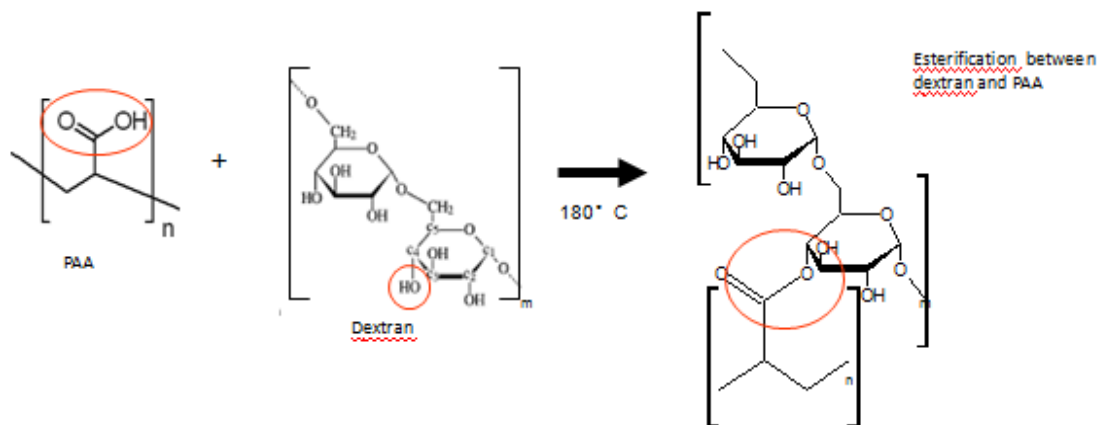


Figure.6 Schematic of Esterification between Dextran and PAA [24]

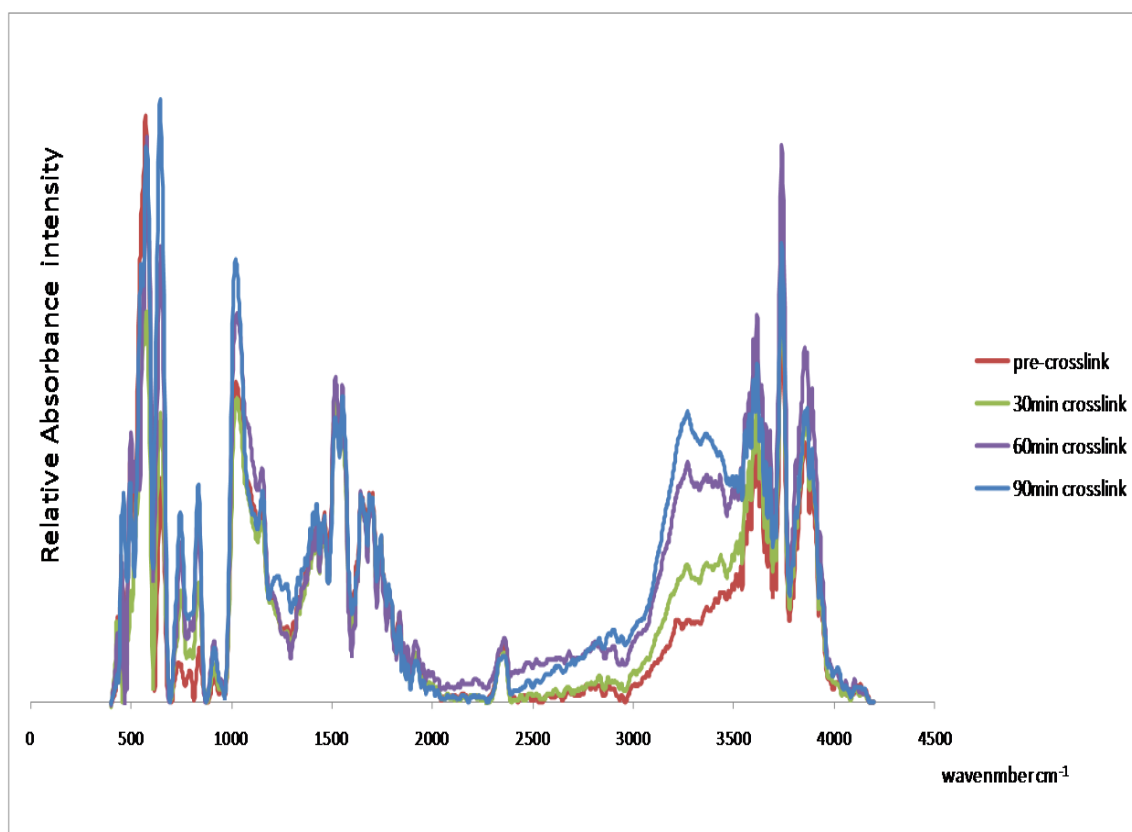


Figure.7 FTIR Spectrum of Dextran-PAA Scaffolds

SWCNT Scaffold Structure Analysis

Scaffolds with different concentrations of single-walled carbon nanotubes were investigated using SEM.

Five polymer solutions with SWCNT concentrations of 0.01%, 0.1%, 0.5%, 1% and 2%, were made for electrospinning. Polymer solution with 2% SWCNT failed to form well-mixed solution and there was serious clog happened after overnight shaking. Polymer solutions with 0.5% and 1% SWCNT could form even distributed solution but failed to make dense fibrous scaffolds (shown in Figure. 8), probably due to the viscosity increase caused by adding SWCNT. Therefore, two scaffolds with SWCNT of 0.01% and 0.1%, as well as control scaffold which contained no SWCNT, were used for SEM imaging and cell seeding tests.

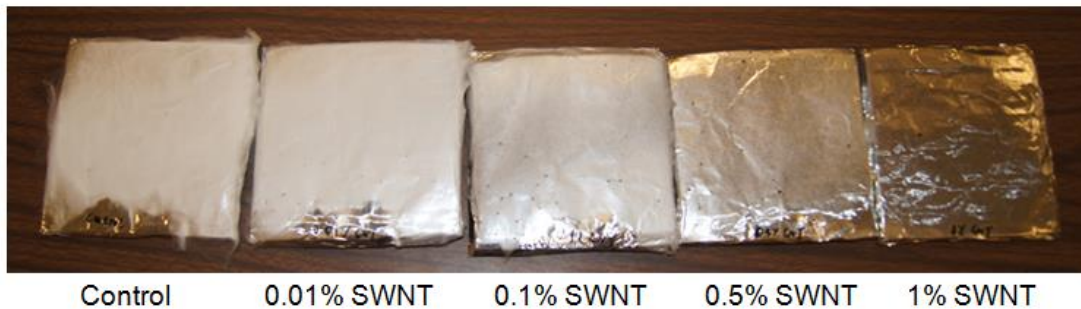
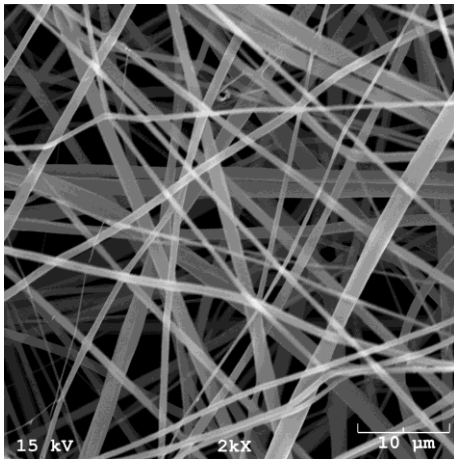


Figure.8 Dextran-PAA Scaffolds with Different Concentrations of SWCNT

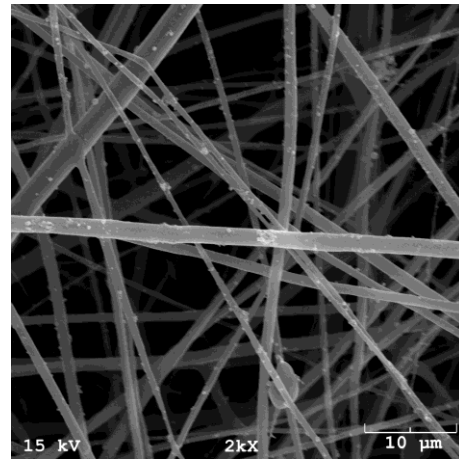
Structures of SWCNT scaffolds, dry state and dehydrated state, were investigated. Dextran-PAA polymer solutions with different concentrations of SWCNT were made for electrospinning. One problem of making SWCNT scaffolds is overcoming SWCNT

agglomeration and obtaining good dispersion of SWCNT in electrospinning polymer solutions. In order to solve this problem, we utilized the ultrasonication to enhance the SWCNT dispersion in polymer solutions. SWCNT aqueous solutions were ultrasonicated before adding them to dextran-PAA polymer solutions. In addition, SWCNT mixed solutions were ultrasonicated again before electrospinning.

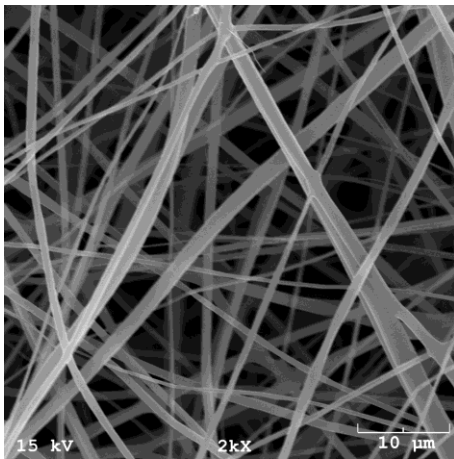
After swelling in water and dehydrated through ethanol and critical point drying, the scaffolds were imaged using SEM (Figure.9). The influence of SWCNT addition is very small to the structure of dextran-PAA scaffolds. After swelling in water, the scaffolds could still keep their porous structures. Figure.9 also shows a structure consistence of scaffolds with different concentrations of SWCNT, so it reasonable to assume that low concentration of SWCNT addition does not cause obviously structure changes of dextran-PAA scaffolds. According to previous research, addition of carbon nanotubes could improve the mechanical stability and stiffness of nanofiber scaffolds, which may potentially be helpful to cell spreading and migration. Based on Figure.9, we can assume that SWCNT was incorporated into the fibers of the scaffolds after electrospinning without changing the porosity and morphology of dextran-PAA scaffolds.



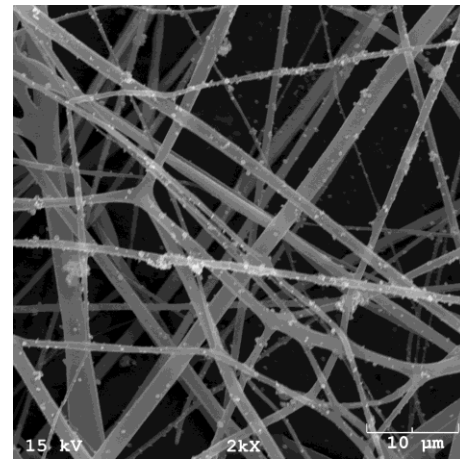
A



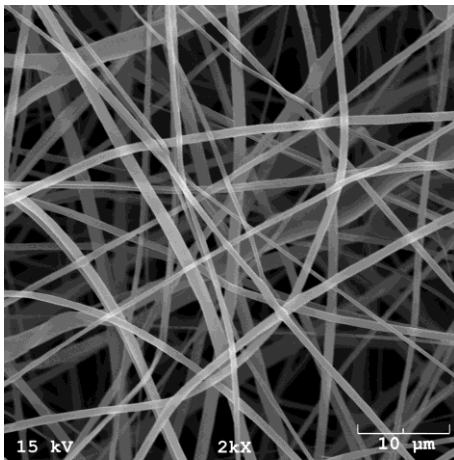
D



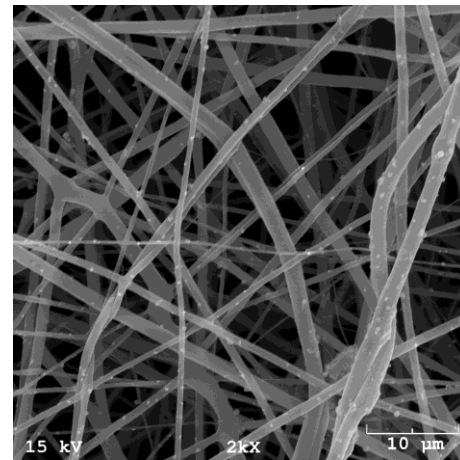
B



E



C

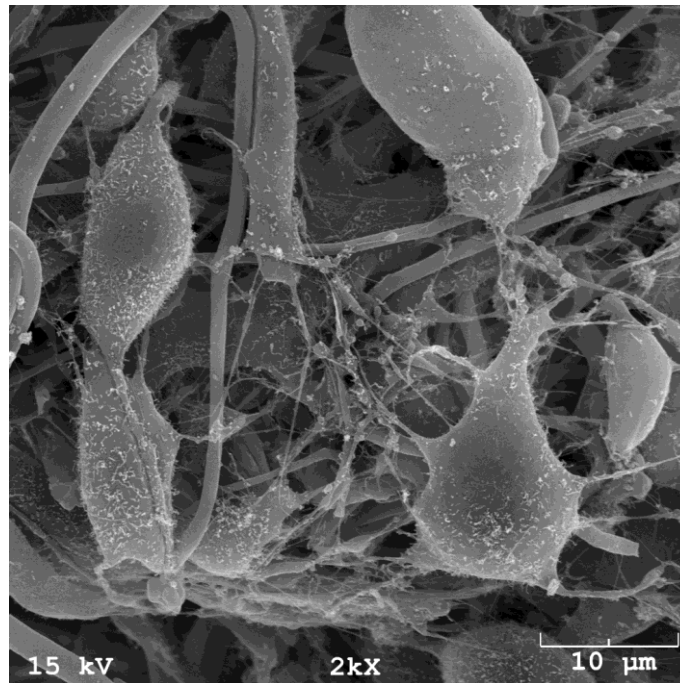


F

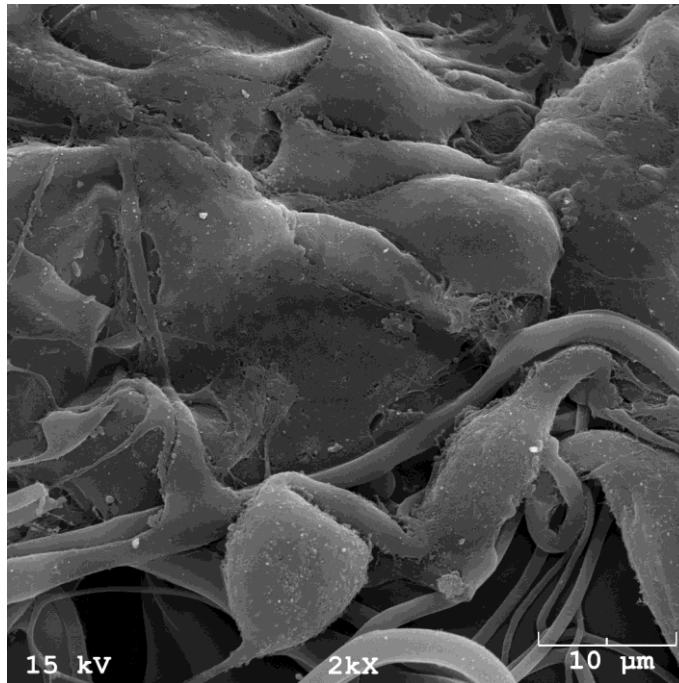
Figure.9 SEM Images of Scaffolds with Different Concentrations of SWCNT
(9 A-C) Dry scaffolds after electrospinning; (9 D-F) Dehydrated scaffolds after
equilibration swelling with water

Cell Response to SWCNT Dextran-PAA Scaffolds

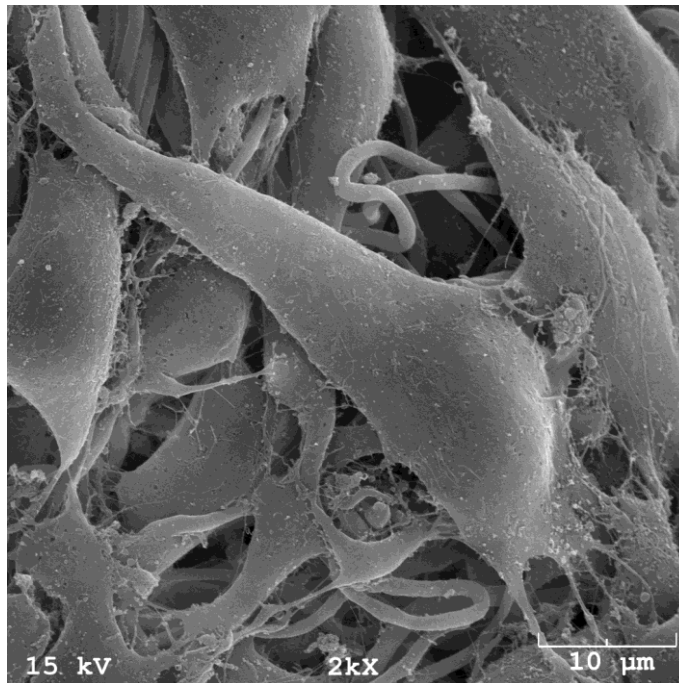
NIH 3T3 fibroblast cells were used in this research to investigate cell affinity of the scaffolds. Cell morphology is a very important indicator to show whether scaffold is bio-compatible to the cells and tissues and whether scaffold could promote cell growth. Three groups of scaffolds, dextran-PAA scaffold, 0.01% SWCNT dextran-PAA scaffold and 0.1% SWCNT dextran-PAA scaffold were seeded with NIH 3T3 fibroblast cells as done previously. 250,000 NIH 3T3 fibroblast cells were seeded onto each scaffold. After 8 days cell culture, the scaffolds were rinsed using PBS and fixed by 2.5% glutaraldehyde, PBS solution. SEM imaging was utilized to observe the cell spreading and distribution the scaffolds.



A. 3T3 fibroblast on dextran-PAA scaffold



B. 3T3 fibroblast on 0.01% SWCNT, dextran-PAA scaffold



C. 3T3 fibroblast on 0.1% SWCNT, dextran-PAA scaffold

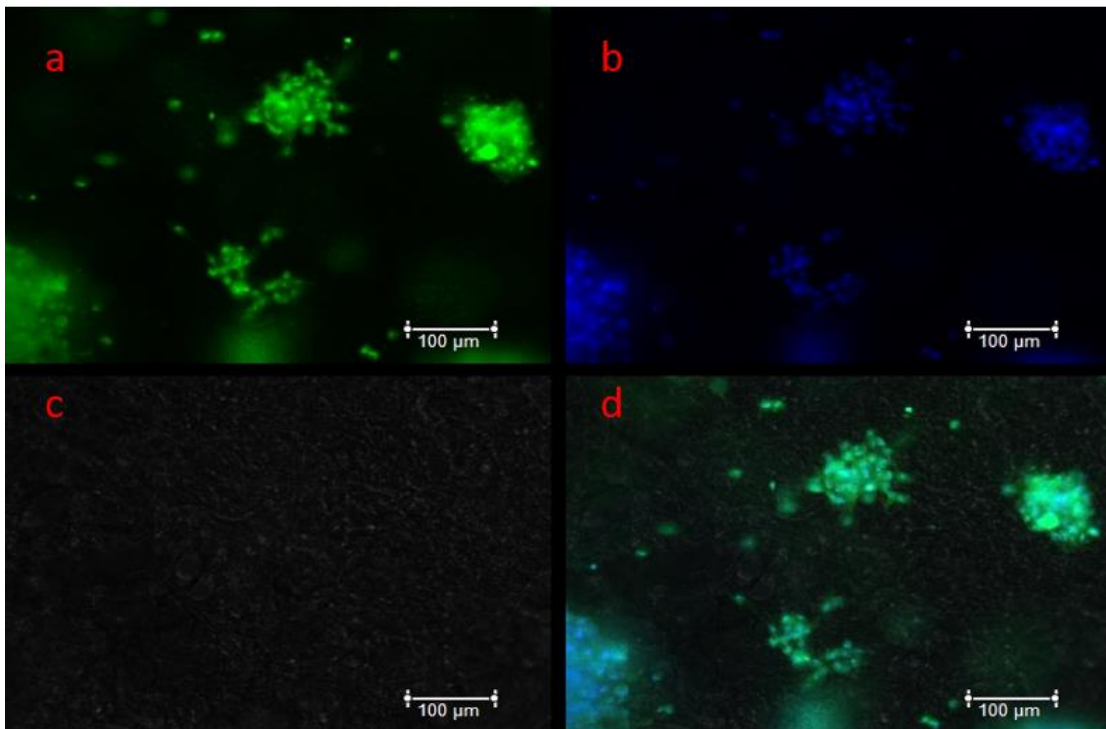
Figure.10 A-C SEM Images of Fibroblast Cells on Dextran-PAA Scaffolds

On Figure.10 A, 3T3 fibroblast cells formed some extracellular connections between each other and some cells expanded along the fibers. But the cell spreading is limited and no cell layer formed. On Figure.10 B, a large number of extracellular contacts can be seen and cell density is very high. A discernable cell layer was formed. On Figure.10 C shows 3T3 fibroblast cells on 0.1% SWCNT dextran-PAA scaffold were fully spread, while on control dextran- PAA scaffold exhibited a less effective spreading and adhesion. Moreover, we can see a large number of connects formed between fibroblast cells. So based on Figure.10 A-C, we can see the increase of SWCNT concentration in dextran-PAA scaffold promoted the 3T3 fibroblast cell distribution and spreading. It suggested that SWCNT reinforced the mechanical properties of fibers in the scaffolds, therefore provided more support and anchorage to cells.

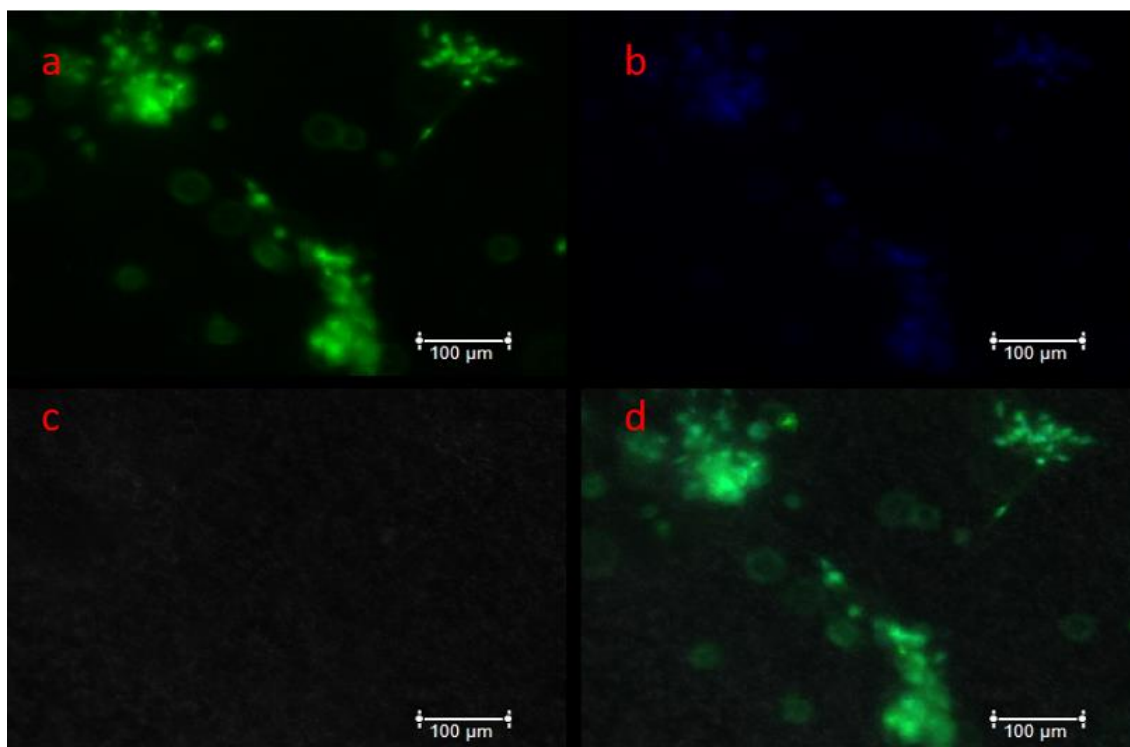
Cell Fluorescence Assay

In order to investigate cell spreading and distribution of 3T3 fibroblast cells on dextran-PAA scaffolds, phalloidin and DAPI were implemented to stain the cells after 8 days culture. Phalloidin can stain filamentous actin within the cytoplasm of cells and DAPI can stain the DNA in the cells. Figure.11 A-C shows the fluorescent micrographs of fibroblast cells on three different scaffolds (Phalloidin (a), DAPI (b), scaffold imaged using DIC microscope (c) and Phalloidin/DAPI/scaffold overlay (d)). After 8 days of *in vitro* culture, the fibroblast cells on the dextran-PAA scaffold (Figure.11 A (a)) were round and had no extensions. Figure.11 A (a) shows cells aggregated together and distributed in several small areas without spreading. On Figure.11 B (a), cell spreading on

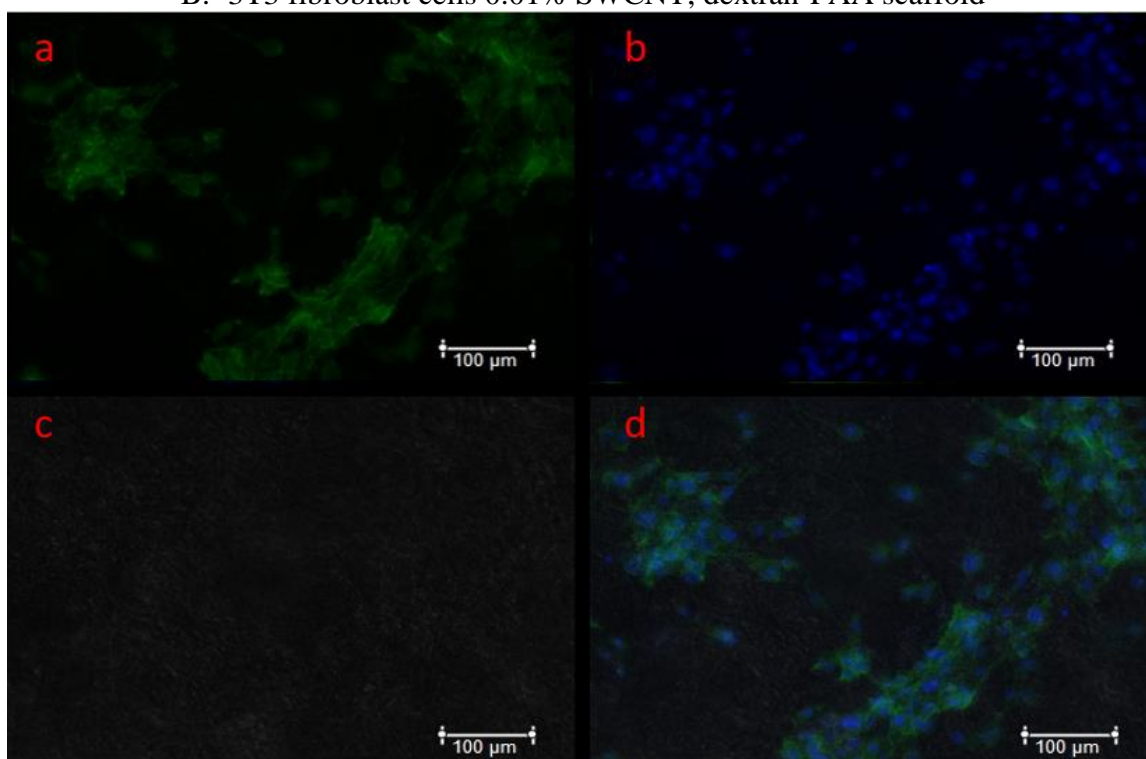
0.01% SWCNT dextran-PAA scaffold got slightly improved. A number of cells began to form extensions, indicating the cells were spreading and forming cell sheets. However, cell distribution on the scaffold was limited (Figure 11. B (b)). On Figure 11 C (a), many cells on 0.1% SWCNT dextran-PAA scaffold were in spindle shape, indicating cell spreading was improved. Most fibroblast cells adhered on 0.1% SWCNT dextran-PAA scaffold surface and exhibited a polygonal and non-stress cell morphology. In addition, cell distribution and sheet formation got discernable improvement on 0.1% SWCNT dextran-PAA scaffold (Figure 11 C (b)). Fibroblast cells covered a large area of scaffold rather than aggregated together, as seen on control and 0.01% SWCNT scaffold.



A. 3T3 fibroblast cells on dextran-PAA scaffold



B. 3T3 fibroblast cells 0.01% SWCNT, dextran-PAA scaffold



C. 3T3 fibroblast cells 0.1% SWCNT, dextran-PAA scaffold

Figure.11 A-C: Fluorescent Images of Fibroblast Cells on Dextran-PAA Scaffolds

Implantation of Scaffolds and Tissue Response Evaluation

Adult female rabbits were used as subjects for dextran-PAA scaffold implantation. Dextran-PAA scaffolds with no SWCNT, 0.01% SWCNT and 0.1% SWCNT were fabricated and wrapped on Surgisis for implantation. One end of Surgisis was marked by suture (Figure.12 A). The color of scaffolds became darker with the increasing of SWCNT concentrations.

The scaffolds wrapped Surgisis grafts were then implanted into the posterior vaginal walls of rabbits. Grafts were removed from rabbits after 14 days (Figure.12 B). Figure.12 B shows that the surrounding tissue on control scaffold is much thinner than the other two scaffolds. Besides, the thickness of tissues increased with the increase of SWCNT concentrations in scaffolds. The tissue samples were then cut vertically along the graft in order to observe the cross-sections of the samples.

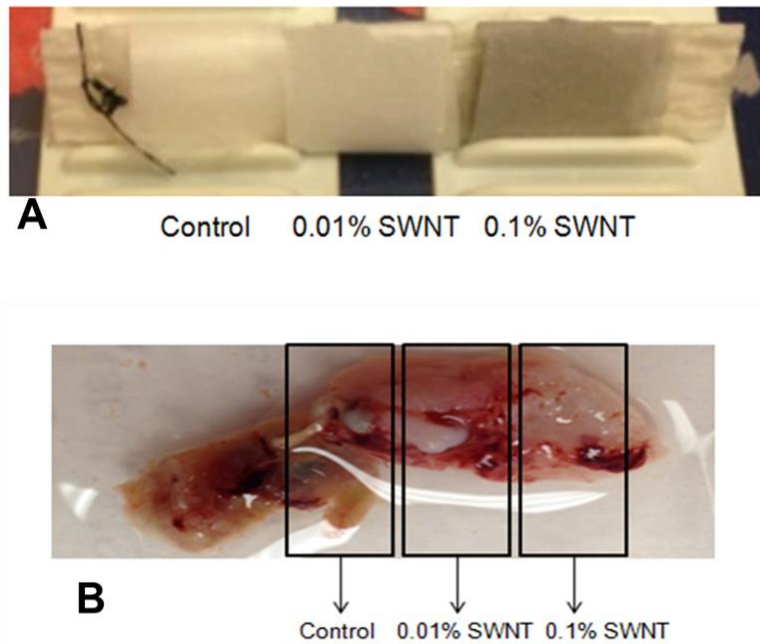
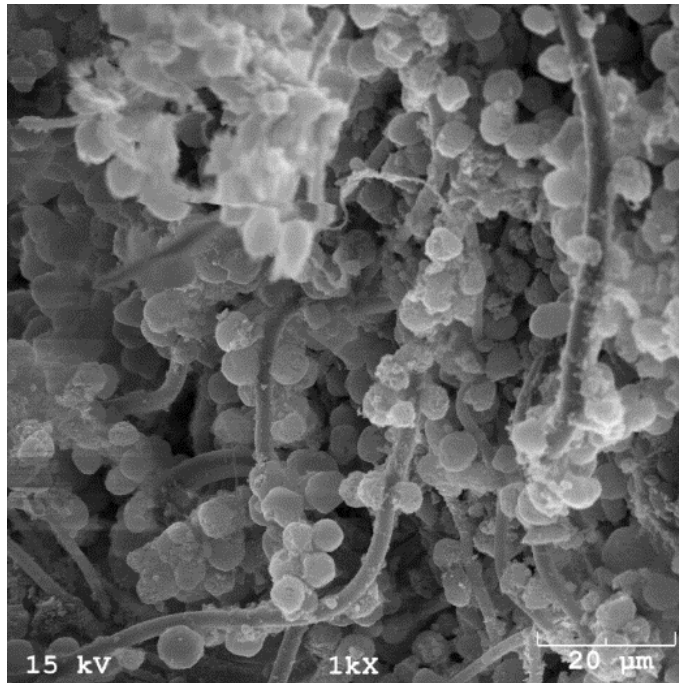


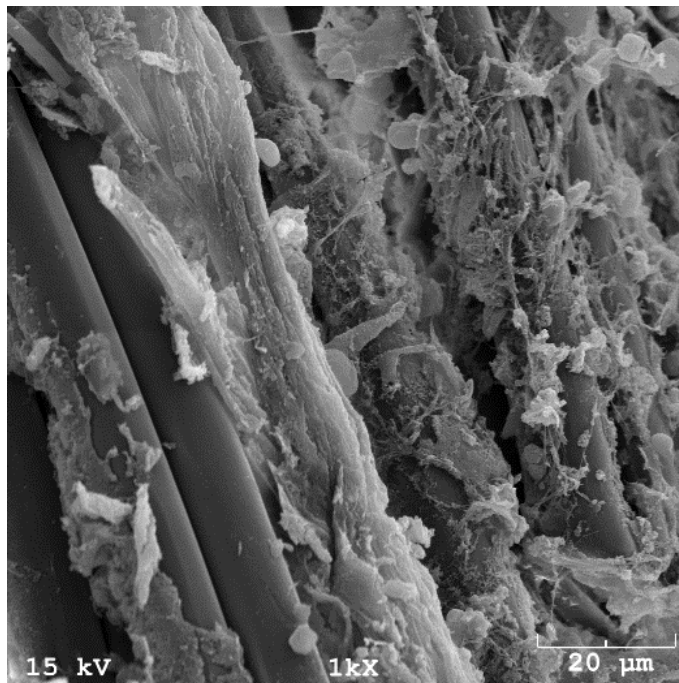
Figure.12 A-B: Scaffolds Wrapped Surgisis Graft before and after Rabbit Implantation

SEM was utilized to observe the cell morphology and proliferation on three different SWCNT concentration scaffolds. Tissues were treated with 5% glutaraldehyde PBS solution overnight at 4°C. Figure.13 A-C shows the rabbit tissue response to the scaffolds after 14 days *in vivo*. On Figure.13 A, cells grown surrounding the fibers of scaffolds mainly maintain round structure. A large amount of fibers are seen that do not have cell coverage. While tissue sample on Figure.13 B demonstrated a good cell spreading condition. Cell coverage on fibers is very high and a large number of cells spread along fibers of scaffolds. On Figure.13 C, most of the fibers are covered by rabbit tissues and extracellular matrix was produced by cells.

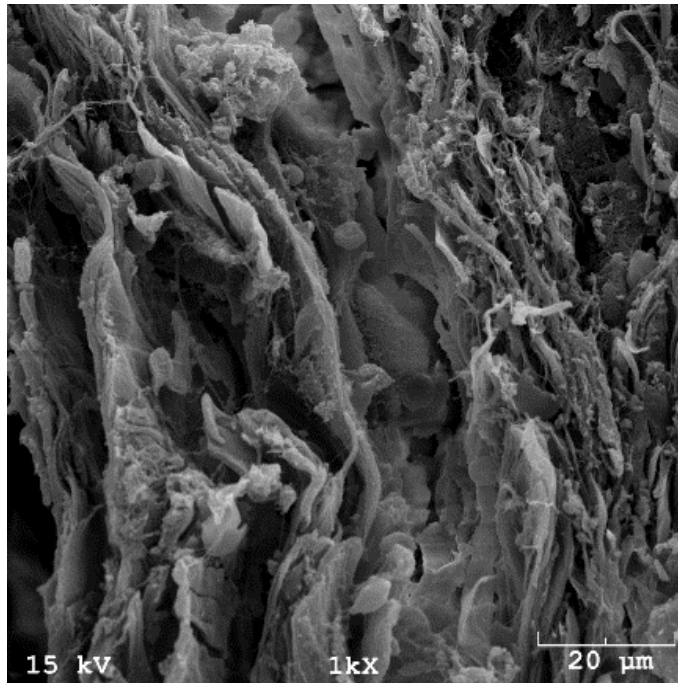
Based on result from Figure.13 A-C, cell density and cell spreading condition were improved with the increasing concentration of SWCNT in dextran-PAA scaffolds. More connective tissue was formed in 0.1% SWCNT dextran-PAA scaffold, which provided more support to the surrounding soft tissues. This result is consistent with the 3T3 fibroblast *in vitro* seeding test.



A. Rabbit tissue on dextran-PAA scaffold (14 days)



B. Rabbit tissue on 0.01% SWCNT, dextran-PAA scaffold (14 days)



C. Rabbit tissue on 0.1% SWCNT, dextran-PAA scaffold (14 days)

Figure.13 A-C: Rabbit Tissue on Dextran-PAA Scaffolds after 14 days Implantation

CHAPTER 5

CONCLUSION

The purpose of this preliminary study is to investigate the function of single-walled carbon nanotube in improving biocompatibility and tissue regeneration of dextran-PAA scaffold and its potential to soft tissue repair applications. SEM and FTIR measurements demonstrated that dextran-PAA scaffold possessed a fibrous physical structure and stable chemical properties, which well mimicked the extracellular matrix of real soft tissues. Cell morphology observation through SEM and fluorescent assay result exhibited that SWCNT adding to dextran-PAA scaffolds improved the cell adhesion, spreading and distribution condition. In addition, rabbit implantation evaluation showed that increasing concentration of SWCNT could enhance tissue proliferation and adhesion, enable the dextran-PAA scaffolds provided more mechanical support to the surrounding tissues.

In conclusion, the long-term stability of dextran-PAA scaffold provides a good support to the cell adhesion. Adding SWCNT potentially improves the interactions of the scaffolds with fibroblast cells and soft tissues, make it easier for the cells to anchor and spread on the scaffolds. In addition, rabbit implantation test also shows tissue regeneration and cell spreading were great improved with increasing concentration of SWCNT.

In this work, the potential of dextran-PAA scaffold for tissue engineering application was investigated. Function of SWCNT to improve the biocompatibility of dextran-PAA scaffold was also successfully proved. All these results demonstrate this dextran-PAA scaffold can be a candidate for soft tissue repair application.

Recommendations for future work:

1. Develop low temperature cross-linking methods for dextran-PAA scaffold fabrication and incorporation of temperature-sensitive biomolecules to further improve cell and tissue responses.
2. Develop mechanical testing platform to quantify scaffold mechanical properties.
3. Further develop fabrication techniques to control scaffold fiber orientation, cross-linking and porosity.
4. Optimize scaffold design for soft tissue regeneration, including implantable POP treatment.

REFERENCES

- [1] Sill T. 2008, Electrospinning: Applications in drug delivery and tissue engineering, *Biomaterials*, 29(33): 1989-2006
- [2] Yarin AL. 2005, Taylor cone and jetting from liquid droplets in electrospinning of nanofibers, *Journal of Applied Physics*, 90(9): 4836-46
- [3] Ding B, Kim H-Y, Lee S-C, Shao C-L, Lee D-R, Park S-J. 2002, Preparation and Characterization of a nanoscale poly(vinylalcohol) fiber aggregate produced by an electrospinning method, *Journal of Polymer Science: Part B: Polymer Physics*, 40: 1261-8
- [4] Kenawy ER, Bowlin GL, Mansfield K, Layman J, Simpson DG, Sanders EH. 2002, Release of tetracycline hydro chloride from electrospun poly(ethylene-co-vinylacetate), poly(lactic acid), and a blend, *Journal of Controlled Release*, 81(1-2): 57-64
- [5] Deitzel JM, Kleinmeyer J, Hirvonen JK, Beck TNC. 2001, Controlled deposition of electrospun poly(ethylene oxide) fibers, *Polymer*, 42: 8163-70
- [6] Biman B. Mandal, Ariela Grinberg, Eun Seok Gil. 2012, High-strength silk protein scaffolds for bone repair, *PNAS*, 109(20): 7699-704
- [7] L. Buttafoco, N.G. Kolkman, P. Engbers-Buijtenhuijs. 2006, Electrospinning of collagen and elastin for tissue engineering applications, *Biomaterials*, 27(5): 724-734
- [8] Kenawy E-R, Abdel-Fattah YR. 2002, Antimicrobial properties of modified and electrospun poly (vunl phenol), *Macromolecular Bioscience*, 2: 261-6
- [9] Liu HQ, Hsieh YL. 2002, Ultrafine fibrous cellulose membranes from electrospinning of cellulose acetate, *J of Polyer Sci Part B: Polymer Physics*, 40: 2119-29
- [10] Morozov VN, Morozova TY, Kallenbach NR. 1998, Atomic force microscopy of structures produced by electro spraying polymer solutions, *International Journal of Mass Spectrometry*, 178: 143-59
- [11] Koombhongse S, Liu WX, Reneker DH. 2001, Flat polymer ribbons and other shapes by electrospinning, *J Polymer Sci: Part B: Polymer Physics*, 39: 2598-606

- [12] Doshi J, Reneker DH. 1995, Electrospinning process and applications of electrospun fibers, *J Electrostatics*, 35(2-3):151–60
- [13] Fong H, Chun I, Reneker DH. 1999, Beaded nanofibers formed during electrospinning, *Polymer*, 40: 4585-92
- [14] Engler AJ, Sen S, Sweeney HL, Discher DE. 2006, Matrix elasticity directs stem cell lineage specification, *Cell*, 126(4): 677-89
- [15] Tan EPS, Lim CT. 2006, Characterization of bulk properties of nanofibrous scaffolds from nanomechanical properties of single nanofibers, *J Biomed Mater Res A*, 77(3): 526-33
- [16] Cirillo G, Hampel S, Spizzirri UG. 2014, Carbon nanotubes hybrid hydrogels in drug delivery: a perspective review, *Biomed Res Int*, 2014: 825017
- [17] Xin Tonga, Jingjing Zhenga, Yancheng Lua. 2007, Swelling and mechanical behaviors of carbon nanotube/poly(vinyl alcohol) hybrid hydrogels, *Material Letters*, 61(8-9): 1704-06
- [19] Chen, H.; Hsieh, Y. L. 2004, Ultrafine hydrogel fibers with dual temperature- and pH-responsive swelling behaviors. *Journal of Polymer Science Part A: Polymer Chemistry*, 42 (24): 6331-6339
- [20] Li, D.; Xia, Y. N. 2004, Electrospinning of nanofibers: Reinventing the wheel? *Advanced Materials*, 16 (14): 1151-70
- [21] Pham QP, Sharma U, Mikos AG. 2006, Electrospinning of polymeric nanofibers for tissue engineering applications: a review. *Tissue Eng*, 12 (5): 1197-211
- [22] Cadee JA, Van Luyn, MJ, Brouwer, LA, Plantinga JA. 2000, In vivo biocompatibility of dextran-based hydrogels, *J Biomed Mater Res*, 50 (3): 397-404
- [23] Yarin AL. 2005, Taylor cone and jetting from liquid droplets in electrospinning of nanofibers, *Journal of Applied Physics*, 90(9): 4836-46
- [24] Louie, Katherine. 2011, Electrospinning of bioactive dex-PAA hydrogel fibers, ASU electronic dissertations and theses, <http://repository.asu.edu/items/9078>

- [25] Smith IO, Liu XH. 2009, Nanostructured polymer scaffolds for tissue engineering and regenerative medicine, Wiley Interdiscip Rev Nanomed Nanobiotechnol, Mar-Apr; 1(2):226-36
- [26] Muhammad Iqbal Sabir, Xiaoxue Xu. 2009, A review on biodegradable polymeric materials for bone tissueengineering applications, J Mater Sci, 44:5713 - 24
- [27] Nuttelman CR, Rice MA. 2008, Macromolecular monomers for the synthesis of hydrogel niches and their application in cell encapsulation and tissue engineering, Prog Polym Sci. 33(2): 167 - 170.
- [28] Walter AJ, Morse AN, Leslie KO, Zobitz ME, Hentz JG, Cornella JL. 2003, Changes in Tensile Strength of Cadaveric Human fascia aata after implantation in a rabbit vagina model. J Urol. 169: 1907 - 1910.
- [29] Walter AJ, Morse AN, Leslie KO, Hentz JG, Cornella JL. 2006, Histologic evaluation of human cadaveric fascia lata in a rabbit vagina model. Int Urogynecol J, 17: 136 - 14

APPENDIX A

DATA COLLECTED MAY 2013- JUNE 2014

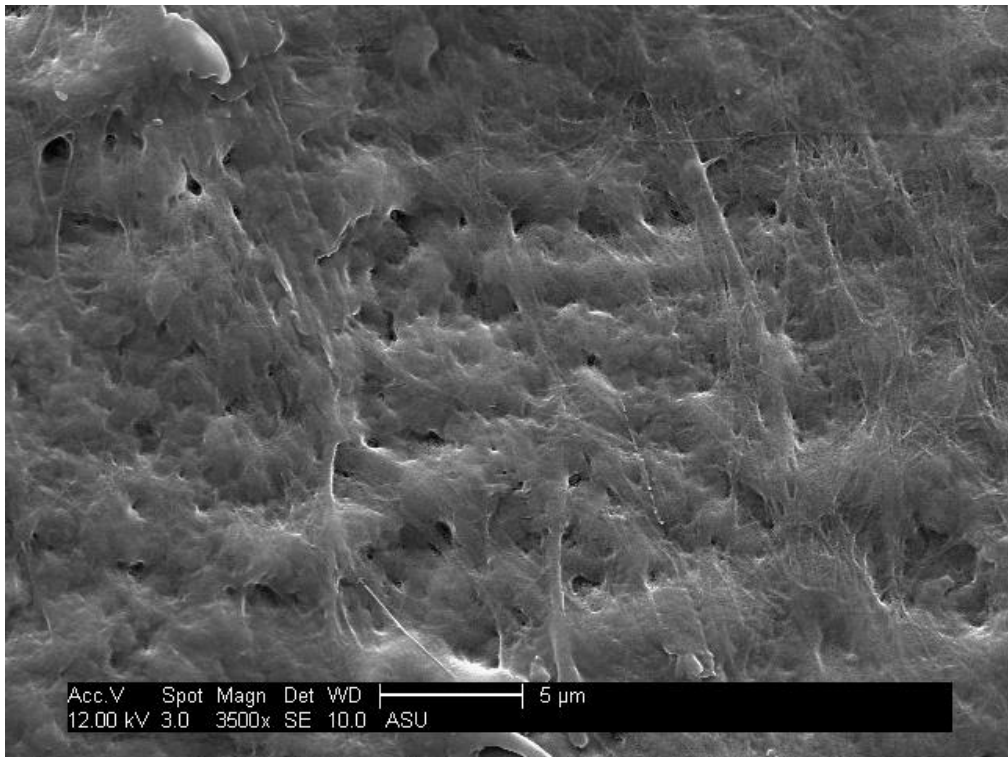
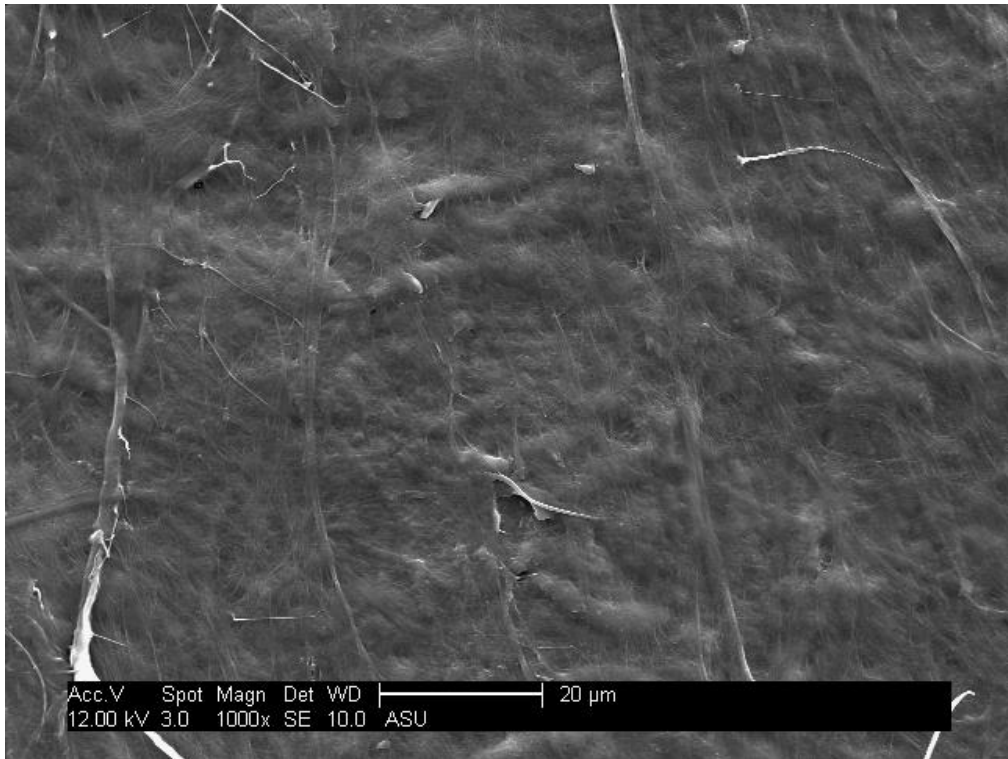


Figure.14 SEM Images of Surgis Graft Surface

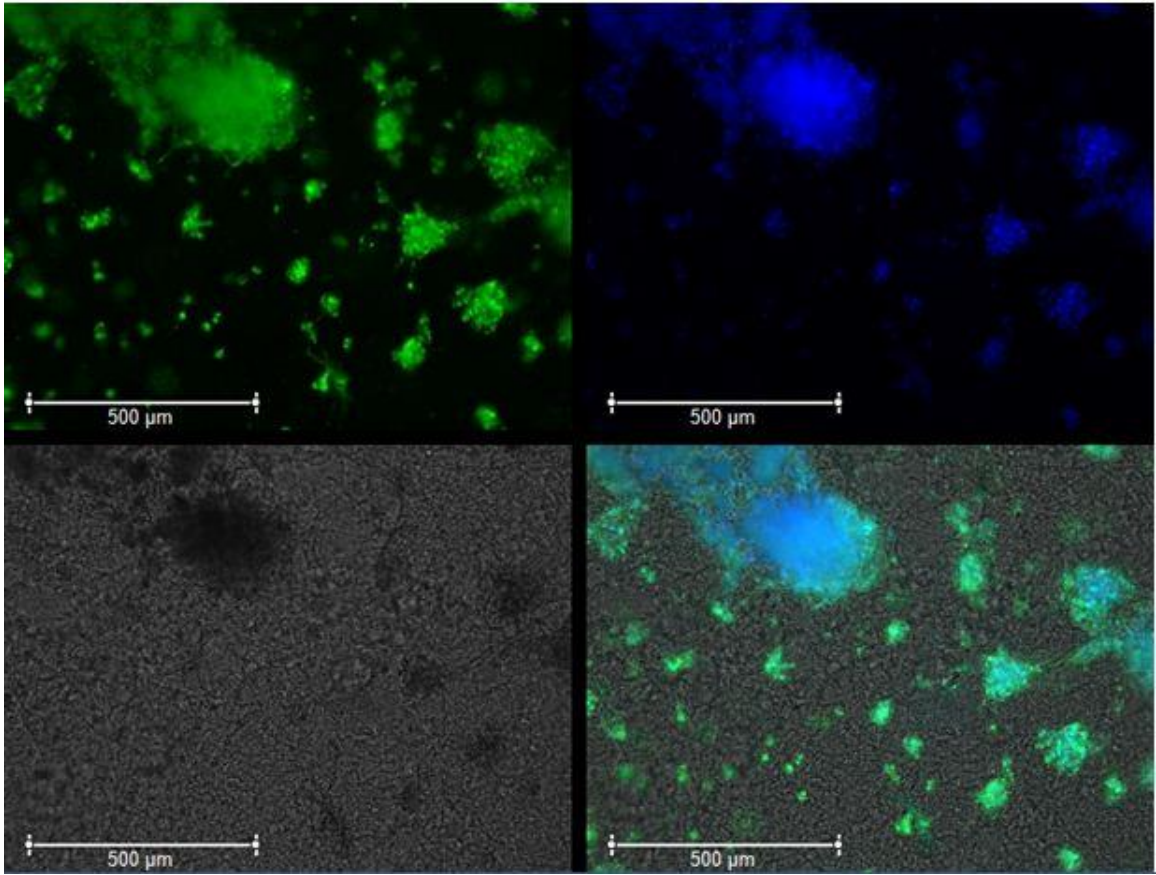


Figure.15 3T3 Fibroblast Cells on Dextran-PAA Scaffold

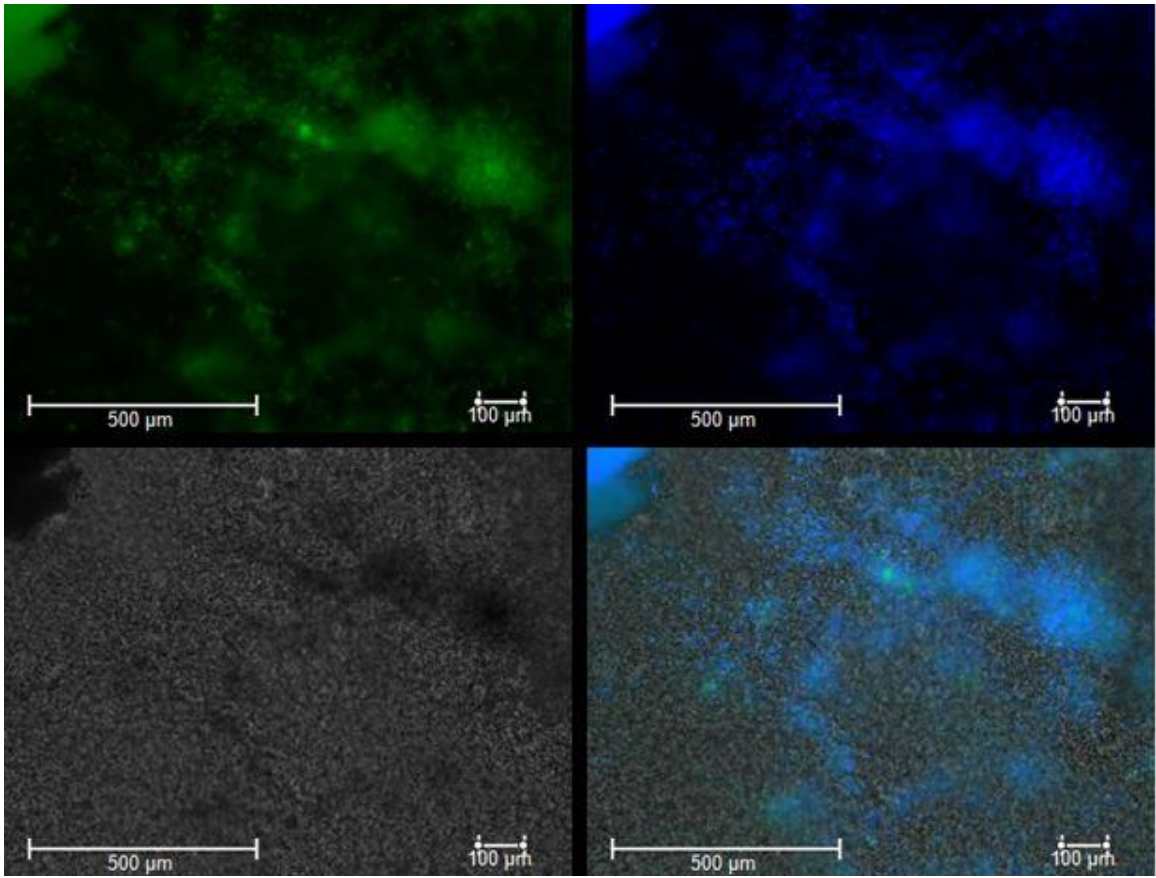


Figure.16 3T3 Fibroblast Cells on 0.01% SWCNT Dextran-PAA Scaffold

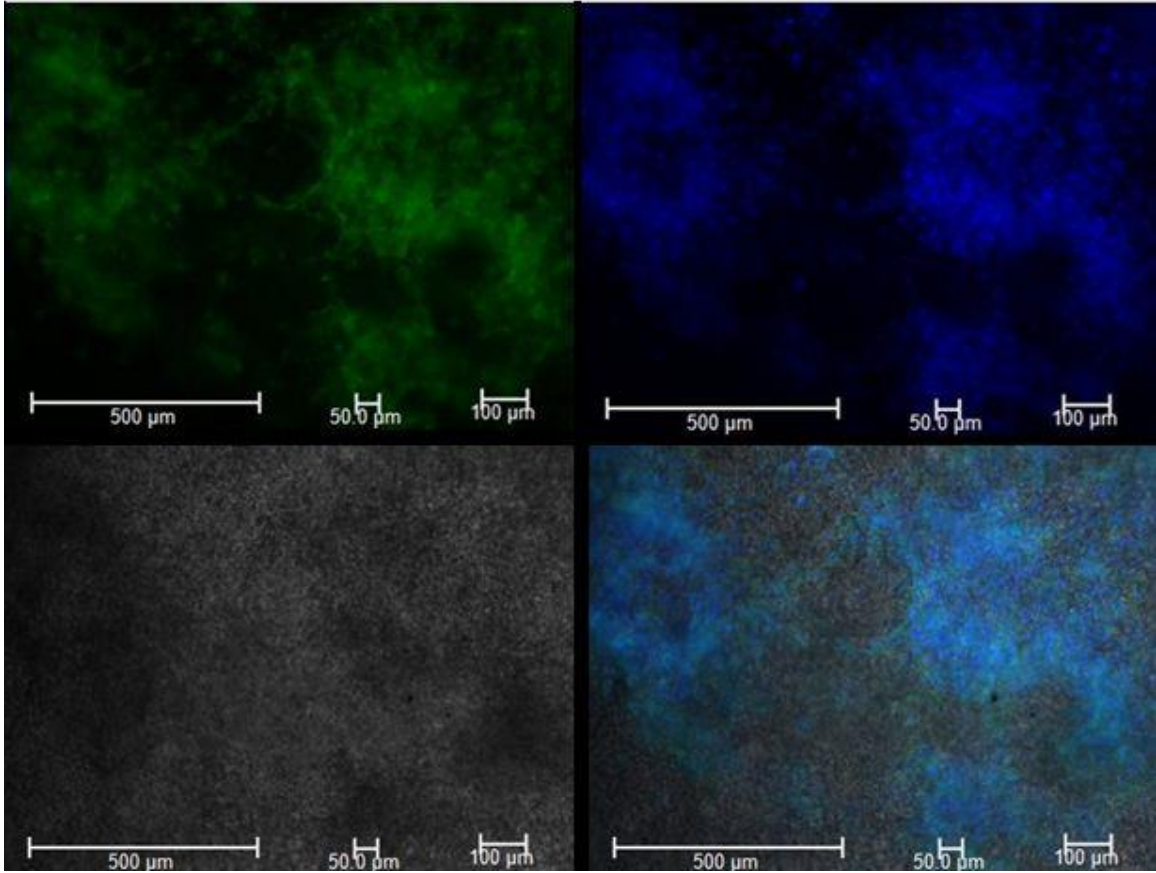


Figure.17 3T3 Fibroblast Cells on 0.1% SWCNT Dextran-PAA Scaffold